Eksploatacja i Niezawodnosc – Maintenance and Reliability
Volume 23 (2021), Issue 3
journal homepage: http://www.ein.org.pl
Article citation info:
Zhao D, Liu Y-X, Ren X-T, Gao J-Z, Liu S-G, Dong L-Q, Cheng M-S. Fatigue life prediction of wire rope based on grey particle filter method under small sample condition. Eksploatacja i Niezawodnosc – Maintenance and Reliability 2021; 23 (3): 454–467, http://doi.org/10.17531/ein.2021.3.6.

Fatigue life prediction of wire rope based on grey particle filter method under small sample condition

Indexed by: Web of Science Group

Dan Zhao [a,*], Yu-Xin Liu [a], Xun-Tao Ren [b], Jing-Zi Gao [a], Shao-Gang Liu [a], Li-Qiang Dong [a], Ming-Shen Cheng [a]

[a] College of Mechanical and Electrical Engineering, Harbin Engineering University, Harbin, 150001, P. R. China
[b] Research Institute 704, China Shipbuilding Industry Corporation, CSIC, Shanghai, 200031, P. R. China

Highlights

- Using high-cycle small sample to predict low-cycle life meets engineering needs.
- Using the grey model to obtain the stress-life curve can reduce test costs.
- The grey particle filter method is proposed to improve the accuracy of P-S-N curve.
- The grey particle filter method is robustness for predicting wire rope's life.

Abstract

The fatigue life prediction of wire ropes has two main characteristics: a large test sample size and uncertain factors. In this paper, based on the small number of wire rope fatigue life data, the grey particle filter method has been used to realize the fatigue life prediction of wire rope under different load conditions. First, the GOM(1,1) model is constructed and the reliability life data of wire rope is predicted under small sample size. Then, P-S-N curve of the dangerous part is determined by combining the equivalent alternating stress of the dangerous part of the wire rope during the fatigue test. Subsequently, the particle filter method is used to modify P-S-N curve. Finally, the fatigue life prediction model of wire rope is obtained based on fatigue damage accumulation, which realized the fatigue life prediction under different load conditions, and the results were compared with that from the test. The results show that the proposed method is effective and has high accuracy in wire rope fatigue life prediction under single, combined loading conditions and small sample size.

Keywords

wire rope, fatigue life prediction, small sample size, grey theory, particle filter method.

Acronyms and Abbreviations

PDF Probability Density Function
CDF Cumulative Density Function

1. Introduction

The wire rope is made by winding the selected steel wire in a certain spiral direction according to the engineering structure and mechanical performance requirements [2]. It is widely used in industrial fields, such as aeronautical engineering, marine engineering, mine industry and port transportation because of high strength, light weight and high reliability [14]. However, the fatigue of wire rope will cause unpredictable risk to life security [19]. Therefore, accurate prediction of the fatigue life of wire ropes in actual engineering is important.

Nowadays, the reliability analysis and life prediction are widely concerned [7, 9, 10, 12], and this paper is aimed to study the fatigue life prediction where the finite element simulation is usually adopted [3]. the fatigue life prediction of wire ropes is mainly dependent on the results of fatigue life test or non-destructive testing. Zhao et al. [21] calculated the fatigue life of the steel wire wound in the rope based on the stress field strength method, and the effectiveness of this method was verified. Wang et al. [18] used three corrosive media as variables to study the fretting fatigue damage of mining steel wire, then combined the wear coefficient to quantitatively analyze the influence of corrosive media on the fretting fatigue life of the steel wire. D. Battini et al. [4] proposed a thermal method for estimating the fatigue life of wire rope through a large number of alternating bending fatigue tests, which has a very good correlation between early data and initial failure conditions. The method leads to a reliable and fast prediction of the number of cycles and the temperature at first wire failure. Wahid et al. [16] divided the fatigue damage process of wire rope into three stages, including the initiate, progressive and brutal damage, and established a damage prediction model using the energy method to accurately predict the tensile fatigue life of wire rope. Based on the above three damage stages, Wahid et al. [17] also characterized the mechanical properties of the wire rope in operation by breaking the strands that constitute the outer layer of the wire rope at different percentages, and predicted the evolution of its damage. Erena et al. [5] studied the fatigue failure of seven-wire stainless steel strands. Through the application of axial load and bending load test combinations and the microscopic analysis of the fracture surface, the results show that the failure is caused by the overall stress rather than fretting. Gordana et al. [8] paid special attention to the creation of parametric 3D CAD model of the seven-wire strand, and explore

(*) Corresponding author.
E-mail addresses: D. Zhao - heuzhaodan@outlook.com, Yu-Xin Liu - 2506660313@qq.com, Xun-Tao Ren - 13564648043@139.com, Jing-Zi Gao - 810410665@qq.com, Shao-Gang Liu - liu_shaogang@hotmail.com, Li-Qiang Dong - dongliqiang@hrbeu.edu.cn, Ming-Shen Cheng - chengmingshen182@163.com

and demonstrate the capacity, performances and difficulties of crack propagation modeling by usage of numerical computational methods in such complex structures. The results show that the finite element method can be used as a powerful auxiliary tool for fatigue life prediction based on tests.

Note that due to the high cost of wire rope fatigue test bench and long test period, it is impossible to have large sample size for fatigue test in engineering practice. Therefore, the steel wire rope fatigue life prediction under small sample size is a challenging. Fortunately, the grey theory can address small sample size problem. It requires fewer samples and easy to use, so it is more applicable [15]. Zhao et al. [20] obtained the low-cycle small sample size data through the fatigue test bench, and realized the high-cycle fatigue life prediction of the wire rope based on the grey theory. Besides, bootstrap is also a data-driven prediction method widely used in small sample research, which can use the existing small amount of data information to imitate the unknown distribution. Mohammad et al. [13] proposed a non-parametric statistical method based on bootstrap for stress analysis of steel bridge components, which can simply and automatically reproduce the complex probability distribution of component fatigue life, and realize the life prediction of steel bridge under small sample conditions. Cao LL et al. [1] extended the smallest sample with the help of bootstrap and evaluated the fatigue reliability of the drive shaft, and finally proved that the method is feasible and reliable for complex structures.

This paper proposes the grey particle filter method, and introduces the particle filter method with powerful parameter estimation. Based on grey theory, the fatigue life of wire rope under small sample size of whole rope test data will be predicted. First, the stress-life curves for the dangerous parts of the wire rope will be determined under sub-samples based on the grey prediction model combined with the equivalent alternating stresses. Then, in order to improve the prediction accuracy, the particle filter method will be used to modify the stress-life curve. Finally, a wire rope fatigue life prediction model will be established based on fatigue damage accumulation to predict the fatigue life under different load conditions.

2. Establishment of the load spectrum of the dangerous part

Determination of the dangerous part of wire rope is the prerequisite for life prediction model, and the fatigue load spectrum is the key to the fatigue life estimation. First, this section uses ANSYS to determine dangerous part of wire rope under actual conditions. According to the wire rope fatigue test data provided by the test bench and dynamic simulation, the equivalent stress-time history curve of the dangerous part is obtained, and then the fatigue load spectrum can be obtained, which is useful for the wire rope life prediction.

2.1. Determination of the dangerous part of wire rope

As shown in Fig. 1, the 6×31WS+FC right-twisted steel wire rope, which includes 6 shares and 31 wires per share, is selected for fatigue test. Its diameter is Φ37mm and the nominal tensile strength is 1960MPa.

The real scene of the bending fatigue test bench is shown in Fig. 2. The wire rope bending fatigue test bench mainly includes fixed and movable pulley components, tensioning mechanism and protective devices. The diameter of the movable and fixed pulleys is 710 mm. When the fatigue test bench is working, the tensioning mechanism exerts a predetermined tensioning force, and the driving mechanism drives the wire rope to reciprocate between the pulleys. The movement period is 15s, and the movement stroke is 1430 mm.

When the broken wire is greater than or equal to 4, the strand is broken or the strand is severely deformed, it can be judged that the wire rope fails, then the test is stopped and the number of reciprocating movements of the rope is recorded currently. Fig. 3 shows actual fracturing part of wire rope obtained from the fatigue test.

(a) Wire rope physical map

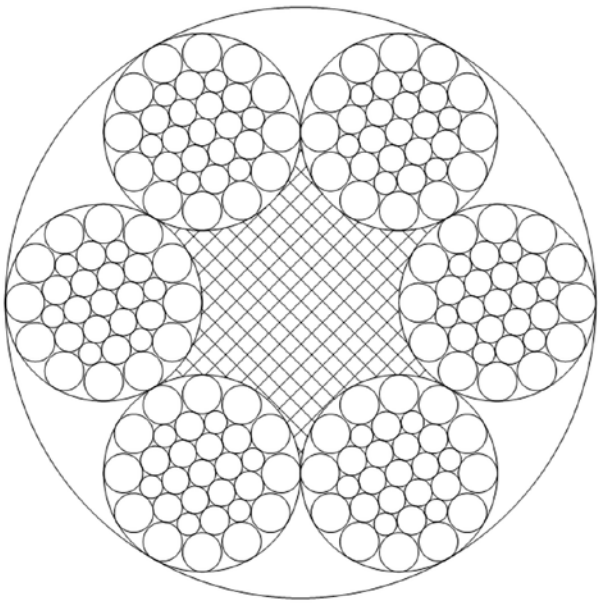

(b) Wire rope section view

Fig. 1. Wire rope for test

Fig. 2. Real Scene of wire rope bending fatigue test bench

The dangerous part of wire rope is analyzed based on the NX10.0 and ANSYS. The 3D model of the wire rope is shown in Fig. 4 and the equivalent stress cloud diagram is shown in Fig. 5.

It can be seen from Fig. 5 that the stress of outermost steel wire in contact between the strands of the wire rope is extremely large, which is the dangerous part of wire rope in the fatigue test and the actual working conditions. Meanwhile, the simulation results are consistent

Fig. 3. Actual fracturing part of wire rope

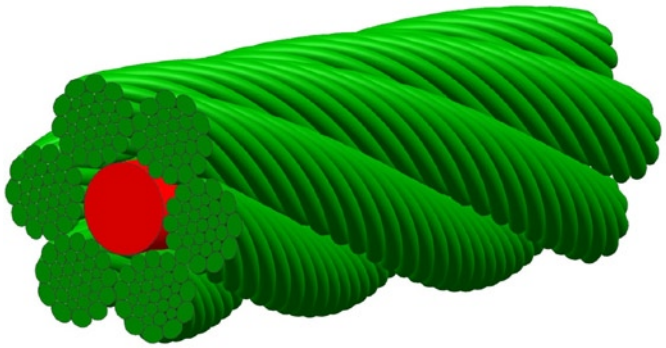

(a) Simple straight line

(b) Curved section

Fig. 4. 3d model of the wire rope

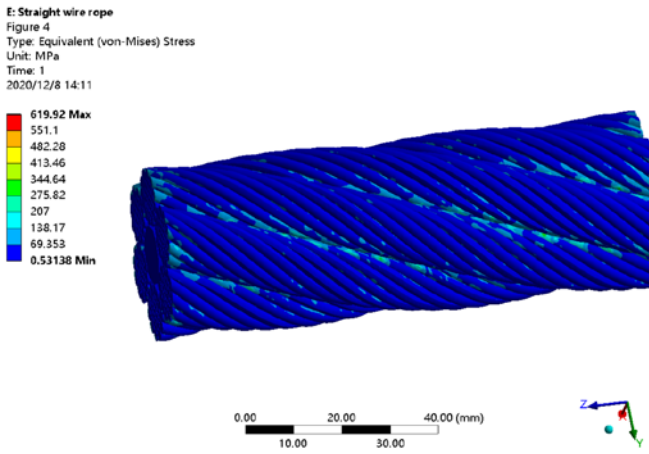

(a) Simple straight line

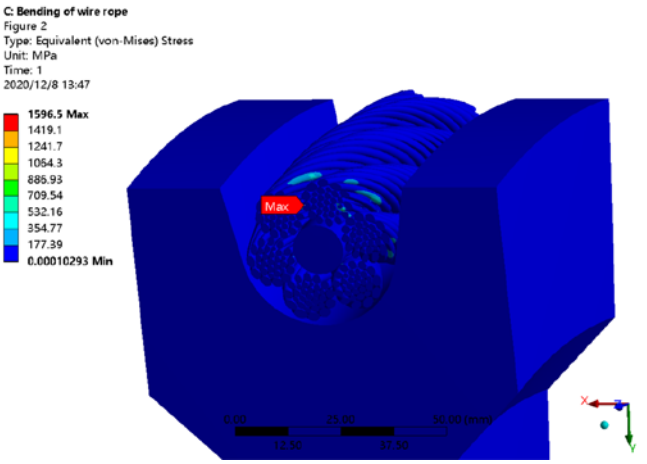

(b) Curved section

Fig. 5. Equivalent stress cloud diagram of steel wire rope

with the actual bending fatigue test, as shown in Fig. 3, which further verifies the accuracy of the simulation.

2.2. Equivalent stress-time history curve of wire rope

During the fatigue test, the wire rope is always subjected to the tensile force and bending moment. In order to simulate the tension, bending and vibration of the wire rope, the ADAMS/Cable module is used to realize the dynamic simulation under different tensions, as shown in Fig. 6. Fig. 7 shows the load-time history curve obtained by simulation, which can be used for load spectrum.

It can be seen from Fig. 7 that the arbitrary point of the wire rope enters and exits the pulley two times in each test cycle, and the bending moment fluctuates cyclically. Due to the small vibration of the

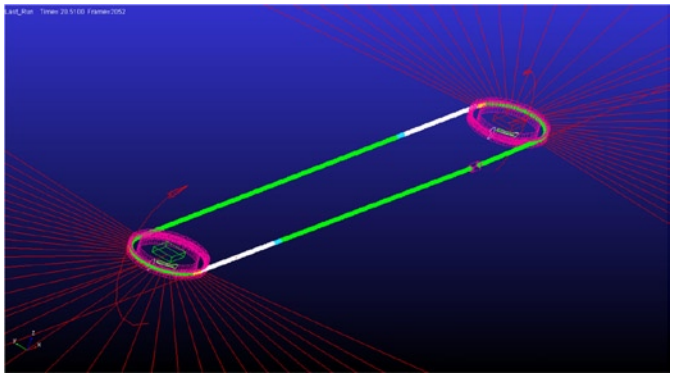

Fig. 6. Dynamic simulation of the wire rope

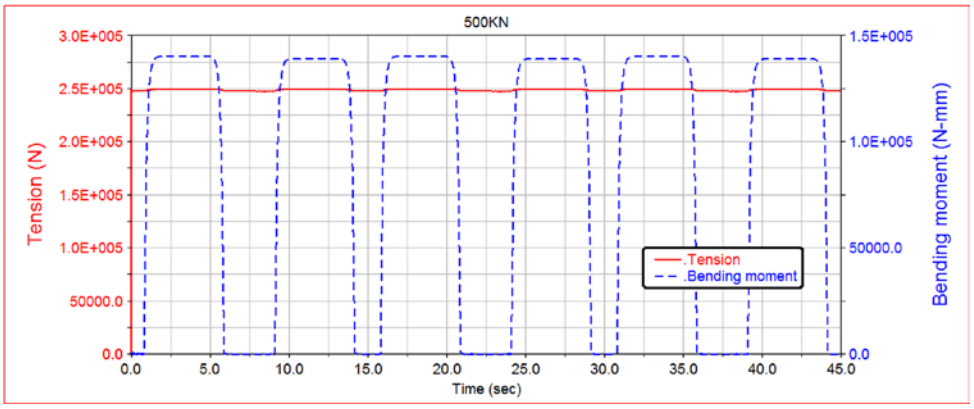

(a) 500kN

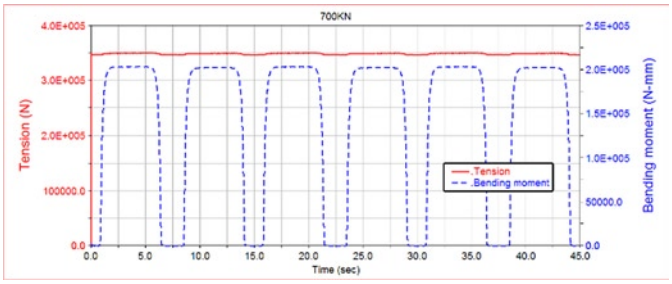

(b) 600kN

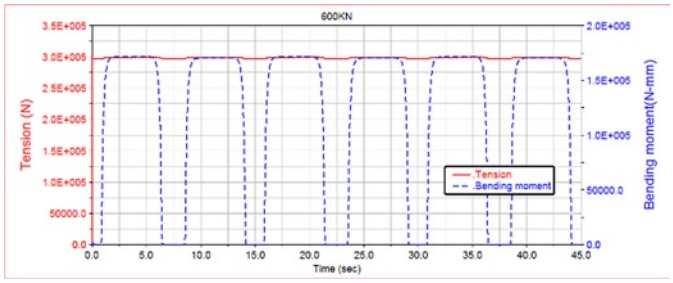

(c) 700kN

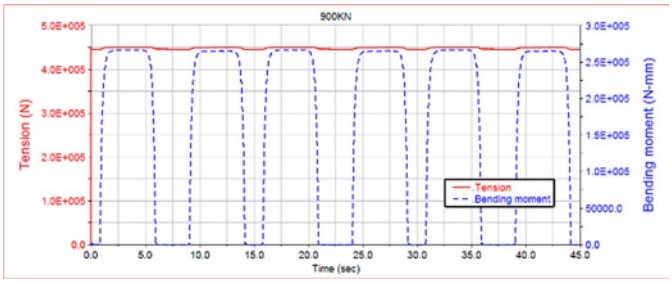

(d) 830kN

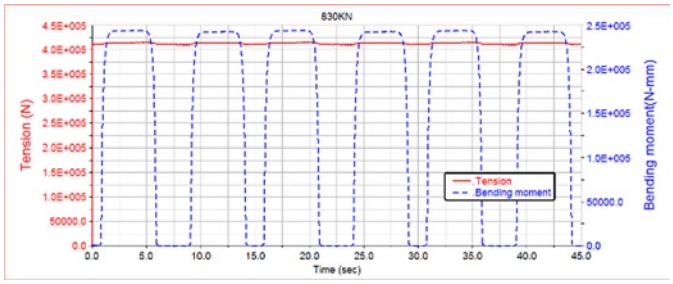

(e) 900kN

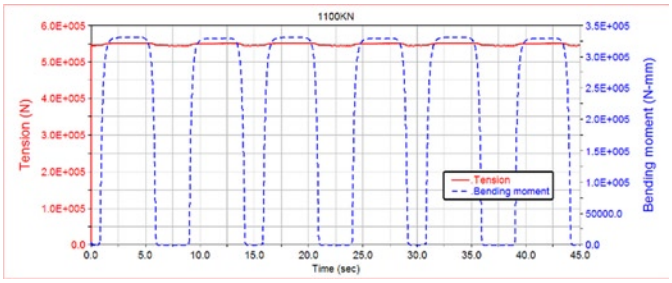

(f) 1020kN

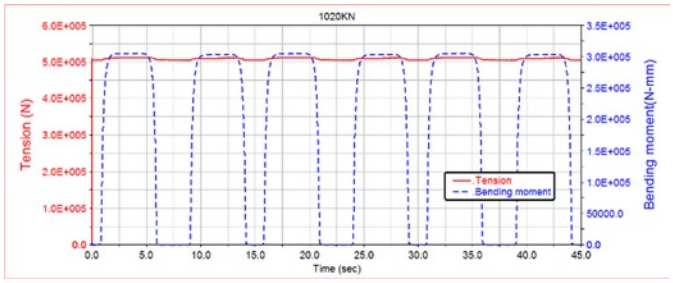

(g) 1100kN

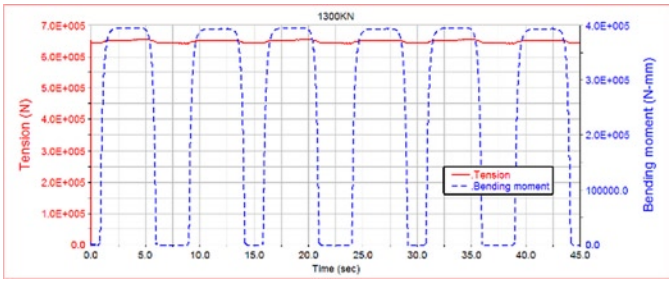

(h) 1200kN

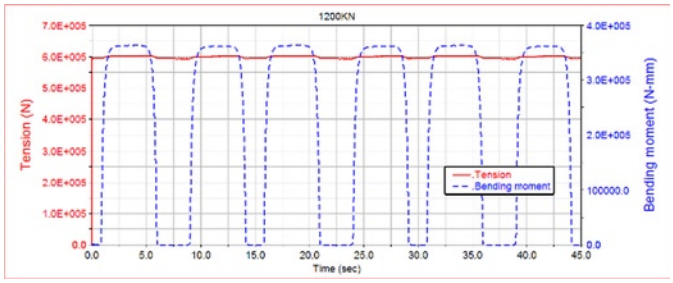

(i) 1300kN

Fig. 7. Load-time history curve under various tension conditions

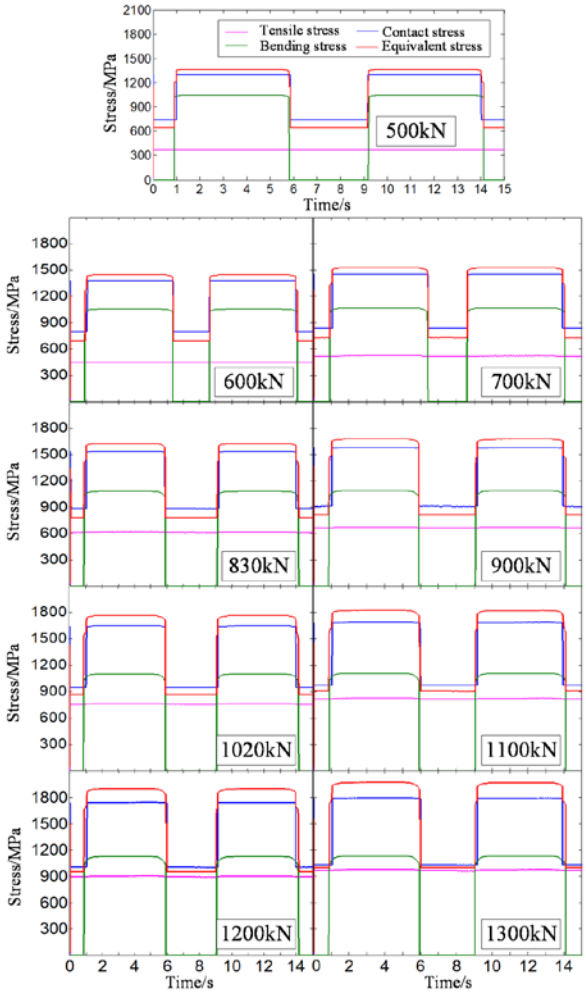

Fig. 8. Stress-time history curve under tension conditions

system, the axial tension of the wire rope changes slightly and irregularly, and the change is obvious in the parts that enters and exits the pulley. However, the overall value is the half of the tension and remains basically stable.

Use the Costello mechanical model to obtain the force expression of the dangerous part, then combine the load-time history curve to have the stress-time history curve of the dangerous part. The results are shown in Fig. 8.

It can be seen from Fig. 8 that when the average value of the cyclic stress on the dangerous part is not 0, the equivalent stress is positively correlated with the tension, and each component stress increases in different degrees with the increase of the tension. Among them, the normal stress, composed of tensile stress and bending stress, and contact stress have similar effects on fatigue in respective uniaxial directions.

2.3. Load spectrum of the dangerous part of wire rope

The rain-flow counting method compiles the stress-time history into the fatigue stress spectrum that causes equivalent damage, which scientifically reflects the memory characteristics of the material, and can effectively simplify the random stress. Rain-flow counting method combines stress-strain hysteresis loop and fatigue damage, and it has advantages in the use of programming to deal with fatigue load and damage calculation problems involving a large amount of cyclic load data. Therefore, its application fields are mainly concentrated on fatigue damage of mechanical parts, vehicle load spectrum, the formulation of aerodynamic fatigue and the calculation of railway fatigue life [11].

The stress-time history under each tension is simplified by rain-flow counting method. The results are shown in Fig. 9.

According to the load selection standard summarized by Heuler et al. [6], the stress cycles whose amplitudes are lower than 20MPa are discarded. The simplified fatigue load spectrum is shown in Table 1.

The stress cycles of actual fatigue damage caused by various tensioning conditions to the wire rope are listed in Table 1. It can be seen that under the working conditions of the test bench, the mean stress and the amplitude are increase with the tension, and both have the same ratio.

Table 1. Simplified load spectrum of the dangerous part of wire rope

Tension (kN)	Mean stress (MPa)	Amplitude (MPa)	Frequency
500	1004	356.4	2
600	1067	377.4	2
700	1128	396.5	2
830	1205	419.6	2
900	1246	430.8	2
1020	1317	448.5	2
1100	1364	457.9	2
1200	1422	473.2	2

Table 2. Equivalent symmetrical cyclic load spectrum of the dangerous part of wire rope

Tension(kN)	Amplitude (MPa)	Frequency
500	730.7	2
600	828.3	2
700	934.1	2
830	1089.3	2
900	1182.6	2
1020	1367.1	2
1100	1505.8	2
1200	1723.9	2
1300	1978.9	2

It is impossible to comprehensively evaluate the influence of the mean stress and the corresponding amplitude on the fatigue life of wire rope. Therefore, after obtaining the load spectrum by rain flow counting method, constructing the Goodman equivalent life curve to convert it into alternating stress of r=-1.

Based on the stress cycle data in Table 1 and Goodman equivalent life curve, the Goodman curve are shown in Fig. 10. It can be seen from Fig. 10 that the stress amplitude of equivalent symmetrical cycle with 1300kN has exceeded the tensile strength to make the wire rope failure quickly, which is consistent to the test life data. The data of vertical axis intersections after sorting is shown in Table 2. Table 2 shows that the equivalent symmetrical stress cycle is affected by the amplitude and average value of the existing stress cycle. When the tension increases, the stress cycle amplitude increases. Since the wire rope fails under 1300kN, this working condition is not considered in this study.

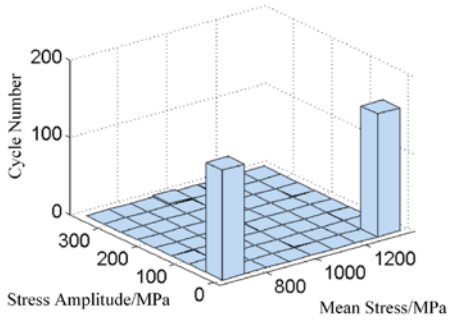

(a) 500kN

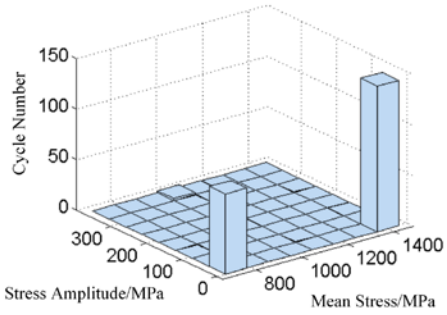

(b) 600kN

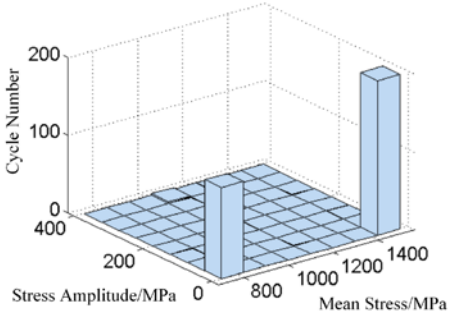

(c) 700kN

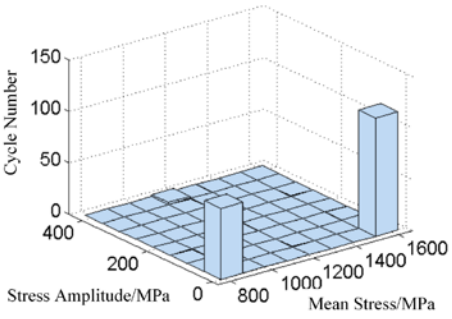

(d) 830kN

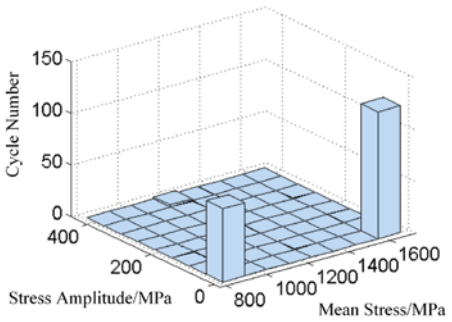

(e) 900kN

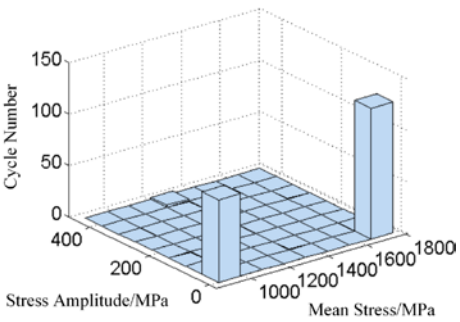

(f) 1020kN

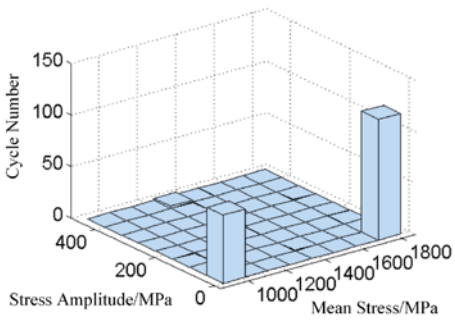

(g) 1100kN

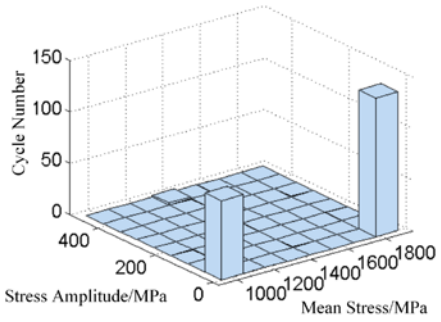

(h) 1200kN

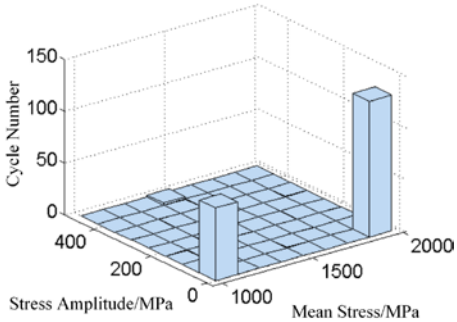

(i) 1300kN

Fig. 9. Load spectrum processed by rain flow counting method

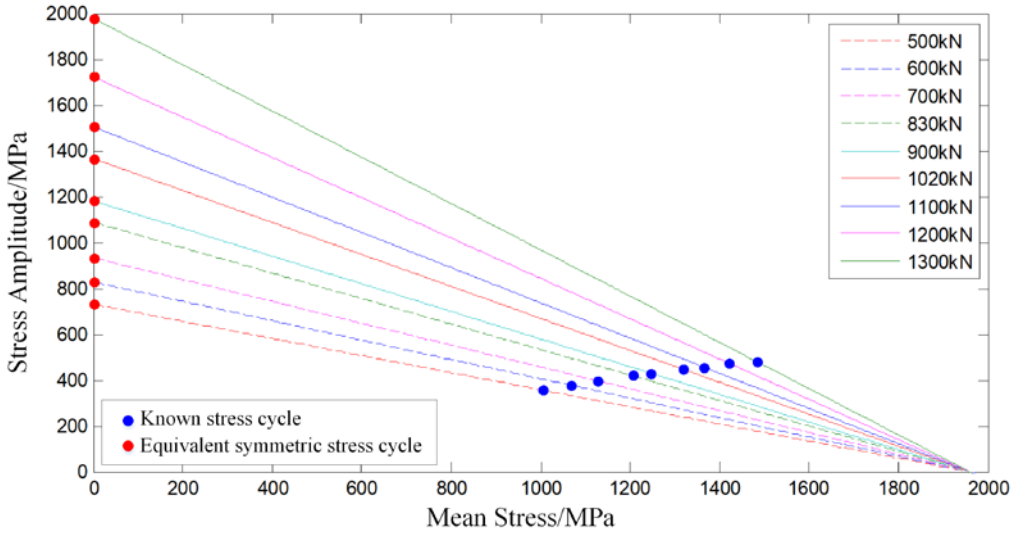

Fig. 10. Goodman curve of stress cycles under various tension condition

3. Analysis of reliable life of wire rope based on small sample condition

The fatigue life prediction model of wire rope is established based on life data. This section first uses bootstrap to regenerate the samples, and then determines the reliability life curve and the life with reliability level of 0.99 under different tensions. Combined with the symmetrical cyclic stress on the dangerous part, the stress-life sequence is obtained.

3.1. Sample regeneration based on Bootstrap

The service life of wire rope follows Weibull distribution [20], which can be expressed as follows:

$$F(N)=1-\exp[-(\frac{N}{\eta})^{\beta}] \tag{1}$$

where, β is shape parameter, η is scale parameter, and N is fatigue life cycle.

Because only four groups of sample data are available from the same tension, the fit test for Weibull distribution is ineffective and the error in estimating the parameters is large. Bootstrap is useful for small sample size and does not have any assumptions about the unknown distribution. Therefore, bootstrap is used for estimating Weibull distribution parameters. The selected test data are shown in Table 3.

Table 3. Fatigue life test data of wire rope

TensionF/kN	*N*
500	15229, 16396, 16793, 17542
600	11217, 11526, 12042, 12371
700	9365, 9861, 10122, 10219
830	8130, 8430, 8550, 9230
900	7340, 7438, 7558, 7935
1020	6331, 6524, 6788, 6824
1100	5168, 5705, 5729, 5891
1200	3369, 4334, 4393, 4401

A sample regeneration using the fatigue test data with 500kN tension condition is considered. 20 regenerated sample data mixed with the 4-original data in ascending order is listed in Table 4.

Fig. 11 shows the results of the Weibull fit test using the data in Table 4. It indicates that the fatigue life data are suitable for Weibull distribution.

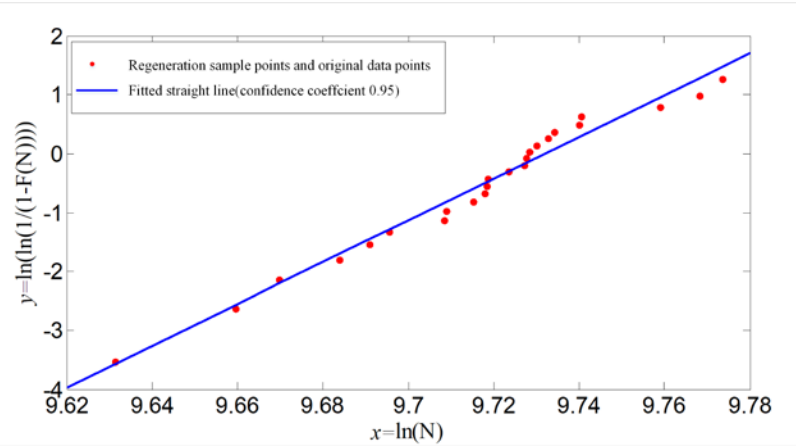

Fig. 11. Weibull test results of regenerated samples under 500kN tension

3.2. Reliability curve of wire rope

Using the fitting straight line method, the parameters can obtain as $\hat{\eta}_0=12107$, $\hat{\beta}_0=33.25$. Fig. 12 shows the probability density function (PDF) and cumulative density function (CDF) of fatigue life.

According to CDF in Fig. 12, the life with reliability level of 0.99 is shown in Fig. 13.

Similarly, the Weibull fitting tests are carried out based on regeneration samples for the remaining tension conditions. The results are shown in Fig. 14 and the fitted parameters are given in Table 5.

The reliability curve with the life under different tension conditions are shown in Fig. 15, and the corresponding life is listed in Table 6.

Table 4. Fatigue life data of wire rope under 500kN tension

Number *i*	Tension *Ni*	Number *i*	Tension *Ni*	Number *i*	Tension *Ni*
1	15229*	9	16566	17	16815
2	15670	10	16610	18	16861
3	15830	11	16618	19	16885
4	16054	12	16626	20	16982
5	16168	13	16704	21	16990
6	16245	14	16765	22	17308
7	16396*	15	16774	23	17469
8	16462	16	16793*	24	17542*

*Remark: The data with * in the table is original data*

3.3. Stress-life sequence for prediction

The symmetrical cyclic stresses at the dangerous parts of the wire rope under different tension conditions are correlated with the reliable life under these conditions to obtain the stress-life sequences for follow-up prediction.

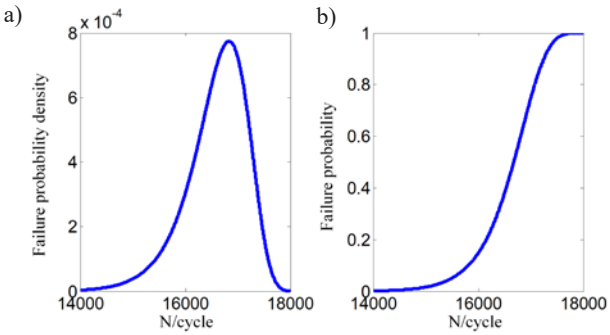

Fig. 12. Curves of failure probability density and failure probability under 500kN tension: (a) Failure probability density curve, (b) Failure probability curve

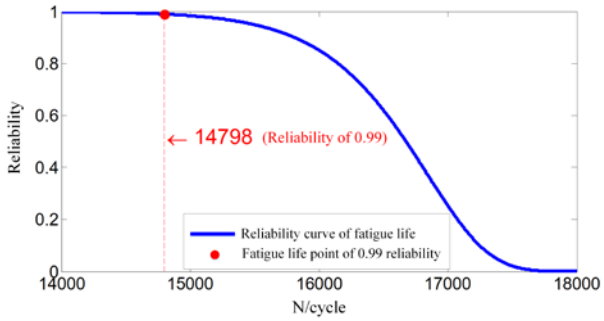

Fig. 13. Reliability curve and the life with reliability level of 0.99 under 500kN tension

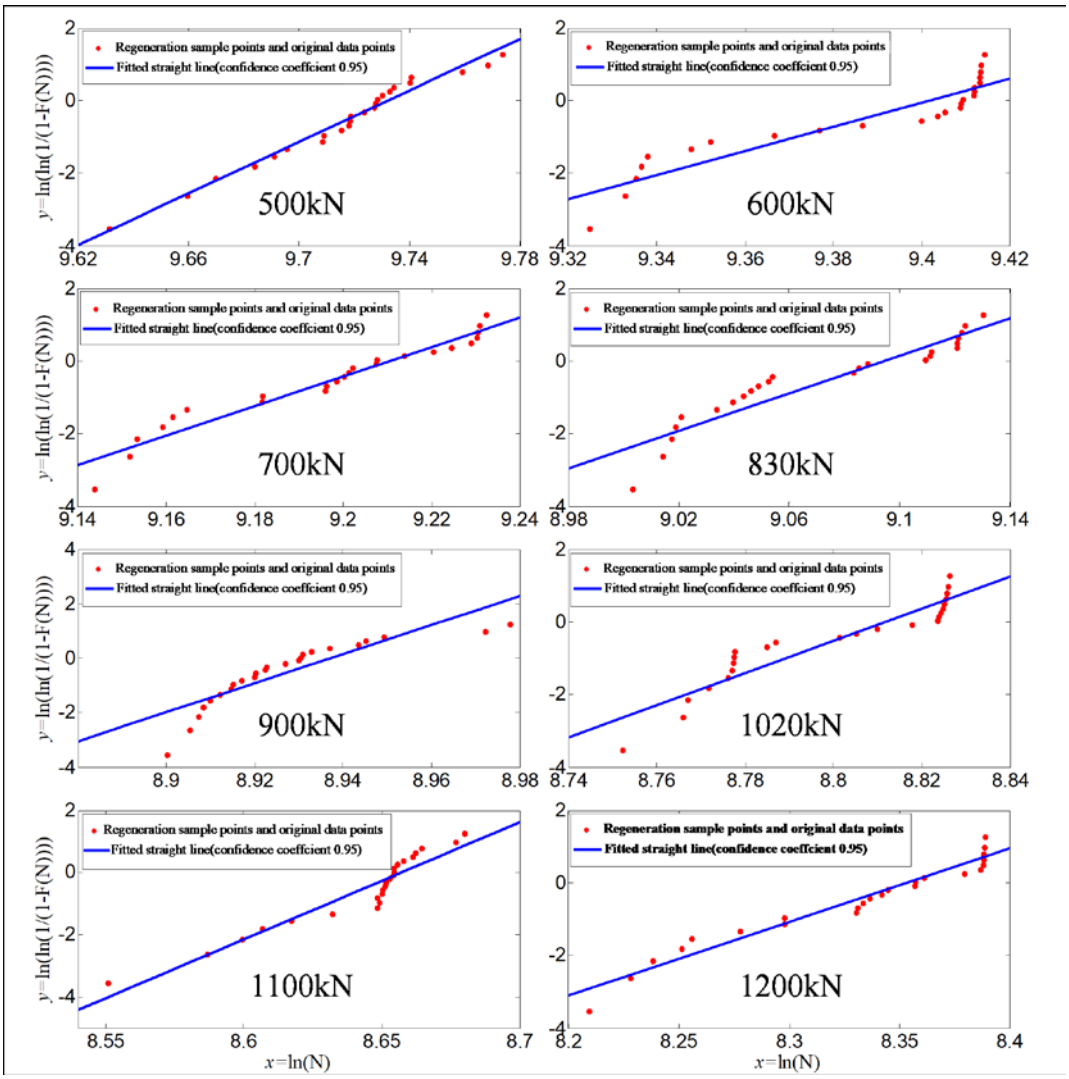

Fig. 14. Weibull fit test results under various tension conditions

Table 5. Weibull distribution parameters for various tension conditions

Tension F`/kN	$\hat{\eta}_0$	$\hat{\beta}_0$
500	16849	35.45
600	12107	33.25
700	10003	40.54
830	8906	25.84
900	7608	53.34
1020	6712	44.35
1100	5751	37.68
1200	4243	20.22

Table 6. the life with reliability level of 0.99 under various tension conditions

Tension F`/kN	N
500	14798
600	10542
700	8930
830	7453
900	6979
1020	6051
1100	5090
1200	3380

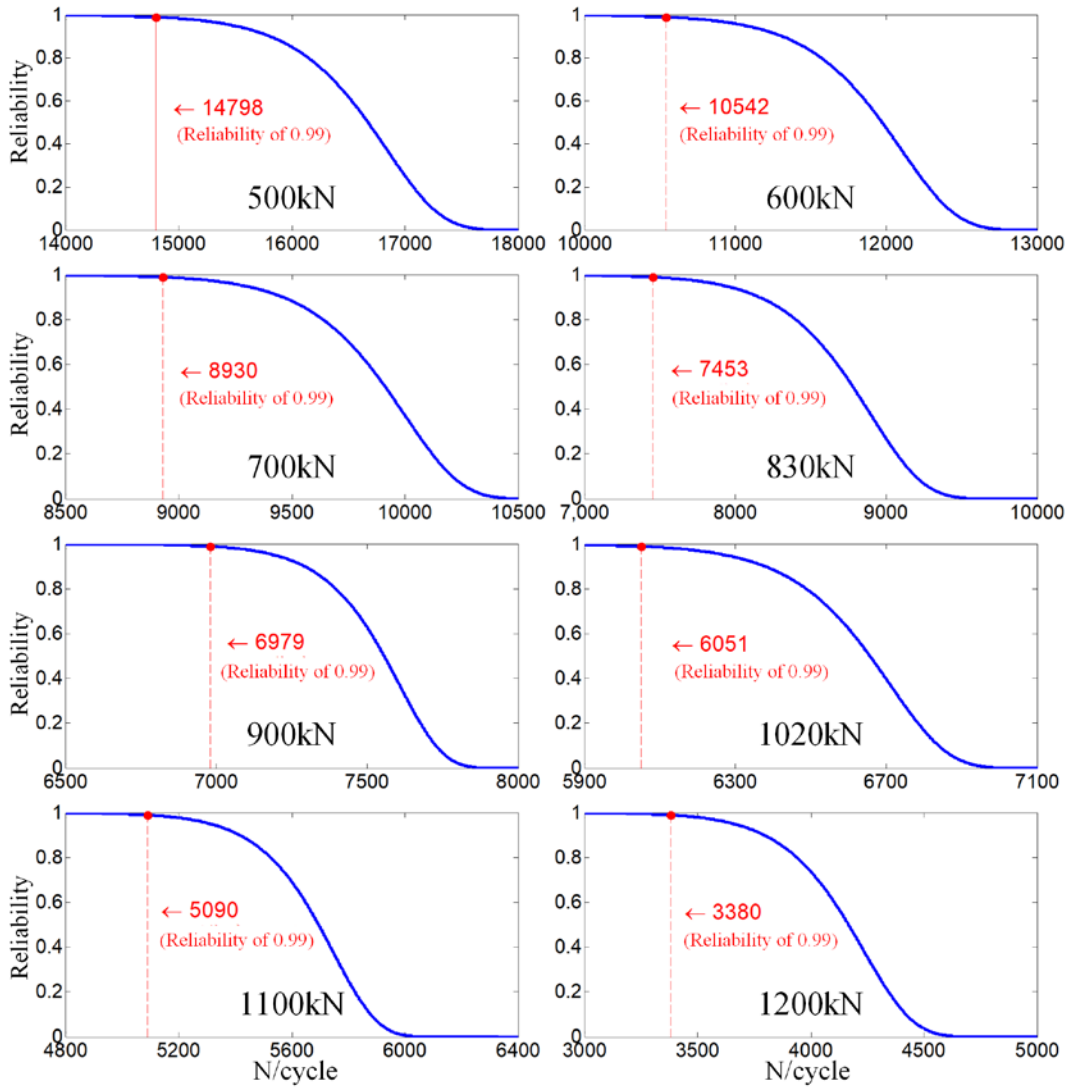

Fig. 15. Reliability curve and the life with reliability level of 0.99 under various tension conditions

Since the fatigue damage suffered by the rope in one stroke on the fatigue test bench is equivalent to the effect of two identical stress cycles, under each tension condition, each stress cycle corresponds to a twice the known life. The corresponding stress-life sequence is shown in Table 7.

4. Fatigue Life Prediction of wire ropes based on the grey particle filter method

4.1. P-S-N curve of the dangerous part of wire rope

Since the initial life data is a monotonically decreasing sequence,

Table 7. Stress-life sequence

Tension F`/kN	Stress σ /MPa	N
500	730.7	29596
600	828.3	22628
700	934.1	17860
830	1089.3	14906
900	1182.6	13958
1020	1367.1	12102
1100	1505.8	10180
1200	1723.9	6790

the non-equidistant GOM(1,1) model is used to predict the fatigue life. The first-order non-isometric GOM(1,1) Whitening Model is given as follows:

$$-x^{(0)}(k_{i-1})+az^{(0)}(k_i)=b \qquad i=2,3,\cdots,n \tag{2}$$

where, $x^{(0)}(k)$ is the original sequence, $z^{(0)}(k)$ is the sequence of original white background value, a is the development coefficient, and b is the grey action quantity.

The least square method is used to identify parameters a and b as follows:

$$\begin{cases} \hat{a}=\dfrac{(n-1)\sum_{i=2}^{n}z^{(1)}(k_i)x^{(0)}(k_{i-1})-\sum_{i=2}^{n}z^{(1)}(k_i)\sum_{i=1}^{n-1}x^{(0)}(k_i)}{(n-1)\sum_{i=2}^{n}z_{(1)}^{2}(k_i)-[\sum_{i=2}^{n}z^{(1)}(k_i)]^2} \\ \hat{b}=\dfrac{\sum_{i=2}^{n}z^{(1)}(k_i)\sum_{i=2}^{n}z^{(1)}(k_i)x^{(0)}(k_{i-1})-\sum_{i=2}^{n}z_{(1)}^{2}(k_i)\sum_{i=1}^{n-1}x^{(0)}(k_i)}{(n-1)\sum_{i=2}^{n}z_{(1)}^{2}(k_i)-[\sum_{i=2}^{n}z^{(1)}(k_i)]^2} \end{cases} \tag{3}$$

The life data from 500kN to 830kN is substituted in Eq. (3) to obtain $a=2.22479\times10^{-3}$, and $b=-1.43624\times10^{4}$. Then, the whitening time-response function of non-equidistant GOM(1,1) model is:

$$\hat{x}^{(1)}(k_i)=[x^{(0)}(k_n)-\frac{\hat{b}}{\hat{a}}]\exp[-\xi\hat{a}(k_i-k_n)]+\frac{\hat{b}}{\hat{a}} \qquad i=1,2,\cdots \tag{4}$$

where, the slope coefficient ξ is 0.88.

The prediction formula of non-equidistant GOM(1,1) model at $\Delta k_i=1$ is:

$$\hat{x}^{(0)}(k_i)=x^{(1)}(k_i)-x^{(1)}(k_{i+1})+x^{(1)}(k_n+1) \quad i=n+1,n+2,\cdots \tag{5}$$

Substituting the result of Eq. (4) into Eq. (5), the P-S-N curve of the dangerous part of wire rope is shown in Fig. 16.

It can be seen from Fig. 16 that the prediction curve fits the first four original data to a higher degree. However, the subsequent prediction errors are large because the dangerous part of the rope enters a low-cycle fatigue phase, and the grey theory cannot be able to obtain regular information beyond the sample points.

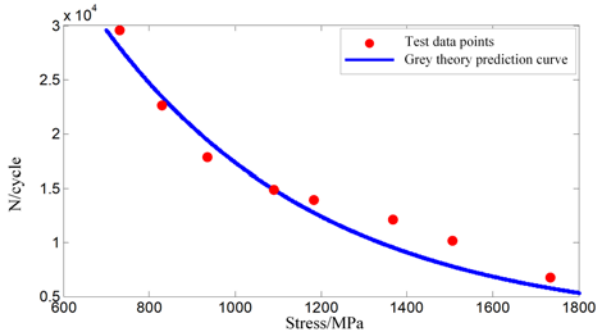

Fig. 16. P-S-N curve of the dangerous part of wire rope

The prediction results and corresponding relative errors are shown in Table 8.

Table 8. Prediction results by non-isometric GOM(1,1) model

Tension /kN	Prediction results	Test results	Relative error
900	12769	13958	−8.52%
1020	9560	12102	−21.00%
1100	7803	10180	−23.35%
1200	5794	6790	−14.67%

4.2. Fatigue life prediction model of wire rope modified based on particle filter method

When the small sample data is in the elastic deformation stage with low loading stress, the grey theory can find the high-circumferential fatigue patterns [21]. The P-S-N curve is revised by applying the plastic strain component of the Manson-coffin formula.

In the low-cycle fatigue phase, it can be considered that the P-S-N curve ignores the plastic strain $\varepsilon_f^{'}(2N)^c$, which can be substituted into the constitutive model of the wire rope to obtain the parameter equations to compensate for the stress component. Since the wire rope often has no obvious yielded point in actual engineering, the stress-strain relationship can be described using a power-hardening model with the following expressions:

$$\sigma=A\varepsilon^n \tag{6}$$

where, ε is the total strain, and n is the power-hardening factor.

Combined with the Manson-coffin formula, the parameter for stress compensation in the low-cycle phase can be obtained as follows:

$$\Delta S=A(\varepsilon_f^{'}(2N)^c)^n \tag{7}$$

where, $\varepsilon_f^{'}$ is the fatigue continuation factor, c is the fatigue continuation index, *and* N is fatigue life.

Eq. (6) represents the distance between the grey theory prediction curve and the test data point on the stress axis. The correction relationship is shown in Fig. 17.

Adding the inverse function of the grey theory prediction formula $S=f^{-1}(N)$ to Eq. (7), combining with the improved four-point correlation method and the formula parameters of steel material, and using MATLAB function *cftool*, S is selected as the horizontal coordinate and N is the vertical coordinate to obtain $N=f(S)+f_2(S)$, the form of grey theoretical predictive formula and modified partial vari-

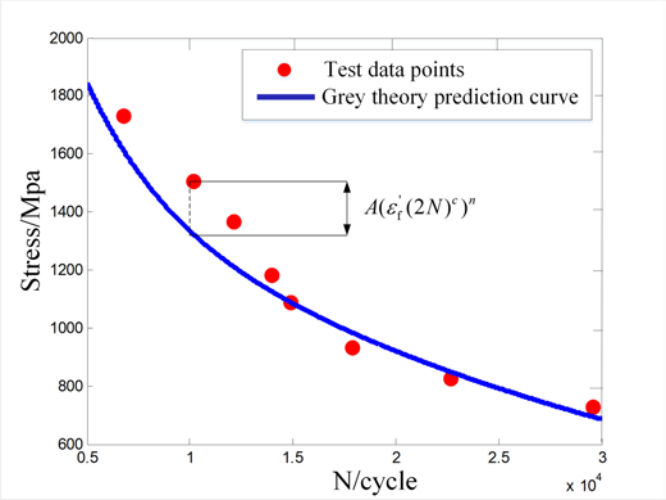

Fig. 17. Correction principle of the grey curve

ant. Among them, the form of $f_2(S)$ is a polynomial of quadratic and above, and considering when the stress of the material in a short-lived zone reaches its own tensile strength, the life will decline rapidly. The inflection points of the measurement are added to the original quadratic polynomial, and the parametric equation is set as:

$$\Delta N = aS^3 + bS^2 + cS + d \tag{8}$$

The parameters a, b, c, d can be solved as follows.

First, the fit is carried out on 4 available test data sets. According to the grey prediction curve, a reliable life of 0.99 corresponding to stresses in the ranges of 700-1100MPa that is selected as the observed true value, and the result is shown in Fig. 18.

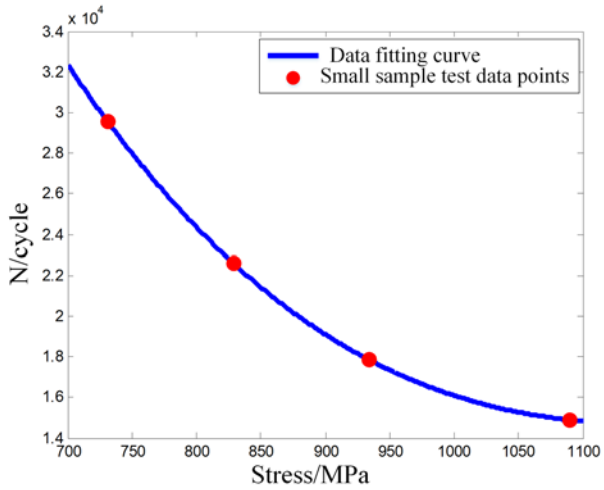

Fig. 18. Effect graph fitting the curve with small sample data

The observation function after fitting is:

$$N = \left(-8.281\times10^{-5}\right)S^3 + 0.3359S^2 - 443.9S + 2.069\times10^5 \tag{9}$$

Treating the parameter values as particles, the state equations are established as follows:

$$\begin{cases} a(k+1) = a(k) + \omega_a \\ b(k+1) = b(k) + \omega_b \\ c(k+1) = c(k) + \omega_c \\ d(k+1) = d(k) + \omega_d \end{cases} \tag{10}$$

where, ω is the Gaussian white noise.

According to the grey theory and measurement equation, we have:

$$N_S = f(S) + a_S S^3 + b_S S^2 + c_S S + d_S + \nu_S \tag{11}$$

where, N_S is the number of alternating stress cycles under stress S, ν_S is Weibull noise under stress S.

Selecting 200 as the number of sampled particles, $S_0 = 1101\text{MPa}$ is the starting point of life prediction, 899MPa is the predicted length, then the multiple particle filtering on the listed spatial equations of state is performed several times. Finally, the modified P-S-N curve is shown in Fig. 19.

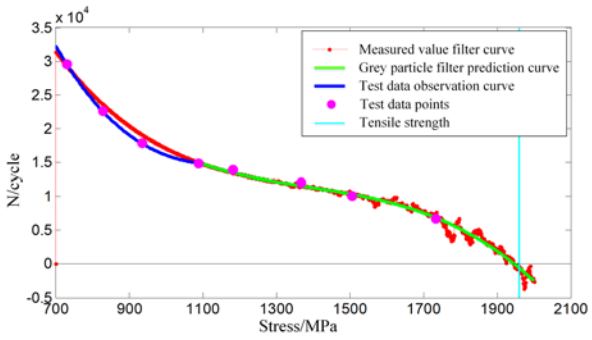

Fig. 19. P-S-N curve modified by grey particle filter

It can be seen from Fig. 19 that the modified prediction model is applicable for small sample data to achieve the wire rope reliable prediction of full-cycle fatigue life. The prediction results and errors for each data point are shown in Table 9. Compared with the life prediction based only on grey theory, the curve trend is almost identical to the actual fatigue behavior of wire rope.

Table 9. The prediction result after grey particle filter's modification.

Tension /kN	Prediction results	Test results	Relative error
900	13442	13958	-3.70%
1020	11582	12102	-4.30%
1100	10384	10180	2.00%
1200	7023	6790	3.43%

The filtering estimation results for a, b, c, and d are shown in Fig. 20. It can be seen from Fig. 20 that the data of each dimension fluctuates slightly after being affected by noise. Thus, the parameter values are set as the average value of each dimension.

$$\begin{cases} a = -3.081\times10^{-5} \\ b = 0.1148 \\ c = -134.9 \\ d = 50550 \end{cases} \tag{12}$$

Substituting the parameters into the measurement equation, the predictive model for the fatigue life based on grey particle filtering is expressed as follows:

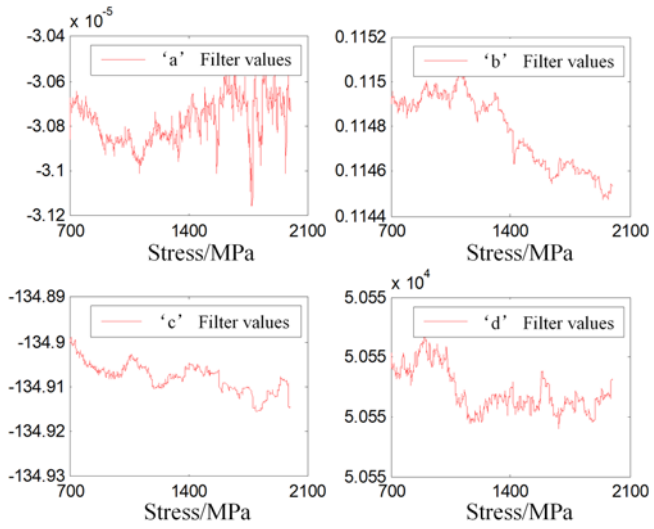

Fig. 20. Filter estimated value of state parameter under a, b, c, d

$$N=\begin{cases}\left(-8.281\times10^{-5}\right)S^3+0.3359S^2-443.9S+2.069\times10^5 \ (\mathrm{S<1100MPa})\\ 109200e^{-0.001978S}+2250e^{-1.878S\times10^{-17}}-3.081S^3\times10^{-5}\\ +0.1148S^2-134.9S+50550 \qquad (\mathrm{S<1100MPa})\end{cases} \tag{13}$$

4.3. Universal applicability analysis of grey particle filter method

The wire rope is often subjected to constant changing tension forces under actual working conditions, and the alternating stress on its dangerous part is changing irregularly. In order to simulate such complex working conditions, a set of combined loading fatigue tests are carried out using the wire rope bending fatigue test bench. The details of loading methods are as follows:

The first phase: 830kN tension for 70 cycles, 1100kN tension for 54 cycles, and 1020kN tension for 76 cycles. The second phase: keeping the first phase until the steel wire rope fails due to fatigue.

The grey particle filter method can predict the fatigue life under single stress. However, for combined loading of multiple tensions, the corresponding load spectrum cannot be equivalently viewed to the single stress cycle spectrum. In order to solve the problems, the existing wire rope life prediction model and Miner theory are combined for combined loading conditions.

The fatigue damage corresponding to each group of stress is calculated by Miner theory, and the results are shown in Table 10.

Table 10. Fatigue damage of each group in combined loading

Tension F_i	Stress S_i	N_i	Fatigue damage D_i	n_i
830	1089	14906	6.709×10^{-5}	140
1100	1506	10384	9.630×10^{-5}	108
1020	1367	11582	8.634×10^{-5}	152

When the cumulative fatigue damage of each group reaches the critical fatigue damage, from the Eq. (13), we have:

$$D=\sum_i D_i\cdot n_i=D_{CR}=1 \tag{14}$$

Then, the total life $N=12172$ is acquired. Converting the existing test reliable life to the single stress cycle, $N_{test}=12426$ can be obtained. The relative error is calculated as:

$$\varepsilon=\frac{N-N_{test}}{N_{test}}=-2.044\% \tag{15}$$

The results show that combined with grey particle filter life prediction model and Miner theory can accurately predict the fatigue life of wire rope under combined loading conditions.

To further demonstrate the high applicability of the proposed model, the fatigue prediction analysis on the other set of wire rope with the tensile strength of 1870MPa is performed. Table 11 shows the fatigue test data when the diameter of the pulley is 700mm. Using the tension-test life data in Table 11, the corresponding symmetrical cyclic load spectrum with reliability of 0.99 is solved. The results are listed in Table 12. The P-S-N curve after grey particle filtering is shown in Fig. 21.

Table 11. Fatigue life test data of wire rope

Tension F /kN	N
700	24618, 24782, 24981, 25681
800	15775, 16105, 16225, 16330
900	9822, 10638, 10874, 11020
1000	6231, 7742, 8967, 9040
1100	3659, 3665, 3702, 3748
1200	2318, 2415, 2541, 2565

Table 12. Test results when the pulley diameter is 700mm

Tension F /kN	σ /MPa	N
700	939.8	24232
800	1061.1	14383
900	1192.4	9154
1000	1341.2	6070
1100	1513.9	3472
1200	1738.1	1884

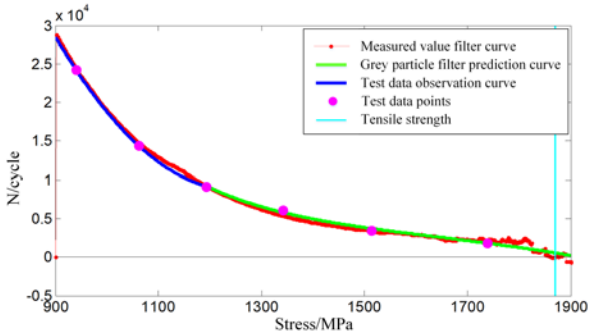

Fig. 21. P-S-N curve of the second set after grey particle filtering

The prediction results and relative errors of each fatigue test data point are shown in Table 13.

It can be seen from Fig. 21 and Table 13 that the P-S-N curves have been more closely aligned with the observed curves. The grey

particle filter prediction model of the second set's fatigue life is obtained as follows:

$$Q=\begin{cases}0.1638S^2-408.9S+2.639\times10^5 & (\mathrm{S}<1200\mathrm{MPa})\\ 1845000e^{-0.004715S}+2470e^{-7.515S\times10^{-17}}-5.969S^3\times10^{-6} & \\ 0.1638S^2-408.9S+2.639\times10^5 & (\mathrm{S}<1200\mathrm{MPa})\end{cases} \quad (16)$$

Table 13. Grey particle filter prediction results and relative errors of the second set

Tension /kN	Prediction results	Test results	Relative error
1000	5839	6070	−3.81%
1100	3746	3472	7.89%
1200	1861	1884	−1.22%

In order to verify that the change of test parameters does not affect the reliability of the prediction model, only the pulley diameter in the test bench is changed to 850mm to predict the fatigue life. The test data of the new condition is given in Table 14:

Table 14. Test results when the pulley diameter is 850mm

Tension F /kN	σ /MPa	N
800	995.6	21325
900	1135.3	12232
1000	1292.5	7368
1100	1473.6	4594

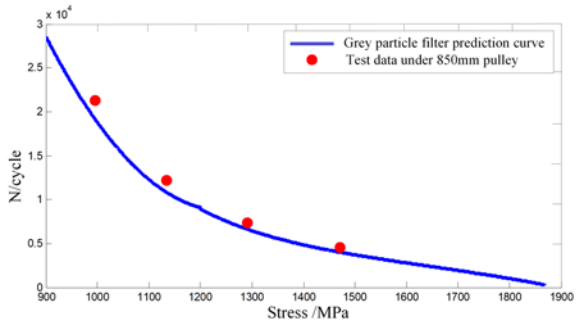

Fig. 22. Prediction of the prediction model under the working condition of 850mm pulley

It can be seen from Table 14 that under the same tension, the fatigue life is significantly improved. The reason is that the pulley diameter increases to make the bending section of the wire rope on the internal contact points increasing, while the contact stress is becoming smaller. Meanwhile, the decrease of curvature of wire rope leads to the decrease of bending stress. Therefore, the equivalent stress of the dangerous part of wire rope is reduced, and the corresponding fatigue life is increased.

Table 15. Relative error analysis when the pulley diameter is 850mm

Tension /kN	Prediction results	Test results	Relative error(max)
800	19211	21325	−9.91%
900	10885	12232	−11.01%
1000	6662	7368	−9.58%
1100	4021	4594	−12.47%

Compared with the test data under the 850mm pulley condition with its P-S-N curve, the result is shown in Fig. 22.

The relative error is listed in Table 15.

It can be obtained from Table 15 that the all relative errors of prediction are smaller than 13%, which meets the high reliability requirements of special wire ropes. Therefore, the grey particle filter method has also high applicability to the fatigue life of wire rope under variable test parameters.

5. Conclusions

For prediction of wire ropes' fatigue life under small sample size condition, this paper proposed the grey particle filter method to predict the fatigue life of the 6×31WS+FC type wire rope. The main conclusions are summarized as follows:

(1) A more accurate P-S-N curve for wire rope is obtained. Compared with the life prediction based on grey theory, the curve modified by the particle filter method is more accurate.

(2) The fatigue life prediction of wire rope under different loading conditions has been realized. The wire rope fatigue life prediction model is established based on the modified P-S-N curve and fatigue damage accumulation, it is used for fatigue life prediction under different loading conditions. The results show that the proposed method has high accuracy for single and combined loading conditions.

(3) The grey particle filter method is robustness. Based on the grey particle filter method, the fatigue life prediction with the tensile strength of 1870MPa is performed and compared with the experimental results. The results show that this method proposed is applicable for fatigue life prediction of general wire ropes.

Acknowledgements

The authors extend sincere gratitude to the National Natural Science Foundation of China for financial support under contract number 51775123.

References

1. Cao LL, Cao LL, Guo L, et al. Reliability estimation for drive axle of wheel loader under extreme small sample. Advances in Mechanical Engineering 2019; 11: 3, https://doi.org/10.1177/1687814019836849.
2. Cao X, Wu WG. The establishment of a mechanics model of multi-strand wire rope subjected to bending load with finite element simulation and experimental verification. International Journal of Mechanical Sciences 2018; 142: 289-303, https://doi.org/10.1016/j.ijmecsci.2018.04.051.
3. Chen Y, Su W, Huang HZ, et al. Stress evolution mechanism and thermo-mechanical reliability analysis of copper-filled TSV interposer. Eksploatacja i Niezawodnosc - Maintenance and Reliability 2020; 22(4): 705-714, https://doi.org/10.17531/ein.2020.4.14.
4. D. Battini, L. Solazzi, et al. Prediction of steel wire rope fatigue life based on thermal measurements. International Journal of Mechanical Sciences 2020; 182, https://doi.org/10.1016/j.ijmecsci.2020.105761.
5. Diego Erena, Jesús Vázquez Valeo, et al. Fatigue and fracture analysis of a seven-wire stainless steel strand under axial and bending loads.

Fatigue & Fracture of Engineering Materials & Structures 2019; 43(1):149-161, https://doi.org/10.1111/ffe.13096.
6. Heuler P, Seeger T. A criterion for omission of variable amplitude loading histories. International Journal of Fatigue 1986; 8(4): 225-230, https://doi.org/10.1016/0142-1123(86)90025-3.
7. Huang T, Xiahou T, Li YF, et al. Assessment of wind turbine generators by fuzzy universal generating function. Eksploatacja i Niezawodnosc - Maintenance and Reliability 2021; 23(2): 308-314, https://doi.org/10.17531/ein.2021.2.10.
8. Kastratovic G, Vidanovic N, Grbovic A, et al. Numerical Simulation of Crack Propagation in Seven-Wire Strand. Computer and Experimental Approaches in Materials Science and Engineering 2020; 90: 76-91, https://doi.org/10.1007/978-3-030-30853-7_5.
9. Li YF, Huang HZ, Mi J, et al. Reliability analysis of multi-state systems with common cause failures based on Bayesian network and fuzzy probability. Annals of Operations Research 2019; https://doi.org/10.1007/s10479-019-03247-6.
10. Li YF, Liu Y, Huang T, et al. Reliability assessment for systems suffering common cause failure based on Bayesian networks and proportional hazards model. Quality and Reliability Engineering International 2020; 36(7): 2509-2520, https://doi.org/10.1002/qre.2713.
11. Liu G, Wang D, Hu Z. Application of the Rain-flow Counting Method in Fatigue. International Conference on Electronics 2016, https://doi.org/10.2991/icence-16.2016.50.
12. Mi J, Li YF, Peng W, et al. Reliability analysis of complex multi-state system with common cause failure based on evidential networks. Reliability Engineering & System Safety 2018; 174: 71-81, https://doi.org/10.1016/j.ress.2018.02.021.
13. Mohammad Reza Saberi, Ali Reza Rahai, Masoud Sanayei, et al. Steel Bridge Service Life Prediction Using Bootstrap Method. International Journal of Civil Engineering 2017; 1A: 51-56, https://doi.org/10.1007/s40999-016-0036-z.
14. Peterka P, Krešák J, et al. Failure analysis of hoisting steel wire rope. Engineering Failure Analysis 2014; 45(1):96-105, https://doi.org/10.1016/j.engfailanal.2014.06.005.
15. Tao YW, He LL, Zhang HW, et al. Research on fatigue life prediction method of tower crane based on grey system. Mechanical Science and Technology 2012; 8: 1236-1240.
16. Wahid A, Mouhib N, Kartouni A, et al. Energy method for experimental life prediction of central core strand constituting a steel wire rope. Engineering Failure Analysis 2018; 97: 61-71, https://doi.org/10.1016/j.engfailanal.2018.12.005.
17. Wahid A, Mouhib N, Ouardi A, et al. Experimental prediction of wire rope damage by energy method. Engineering Structures 2019; 201. https://doi.org/10.1016/j.engstruct.2019.109794
18. Wang D, Zhang D, Zhao W, et al. Quantitative analyses of fretting fatigue damages of mine rope wires in different corrosive media. Materials Science & Engineering A 2014; 596(4): 80-88, https://doi.org/10.1016/j.msea.2013.12.047.
19. Zhang D, Feng C, Chen K, et al. Effect of Broken Wire on Bending Fatigue Characteristics of Wire Ropes. International Journal of Fatigue 2017; 103: 456-465, https://doi.org/10.1016/j.ijfatigue.2017.06.024.
20. Zhao D, Gao CX, Zhou Z, et al. Fatigue life prediction of the wire rope based on grey theory under small sample condition. Engineering Failure Analysis 2020, 107(SI), https://doi.org/10.1016/j.engfailanal.2019.104237.
21. Zhao D, Liu SG, Xu Q T, et al. Fatigue life prediction of wire rope based on stress field intensity method. Engineering Failure Analysis 2017; 81: 1-9, https://doi.org/10.1016/j.engfailanal.2017.07.019.